

Magnetosonic Mach number effect of the position of the bow shock at Mars in comparison to Venus

N. J. T. Edberg,^{1,2} M. Lester,¹ S. W. H. Cowley,¹ D. A. Brain,³ M. Fränz,⁴
and S. Barabash⁵

Received 16 October 2009; revised 26 November 2009; accepted 17 December 2009; published 3 July 2010.

[1] We study the effect of the magnetosonic Mach number on the position of the bow shock (BS) at Mars. The magnetosonic Mach number is calculated from solar wind data obtained by the ACE satellite upstream of Earth and extrapolated to Mars during two intervals, starting in 2005 and 2007, when Mars and Earth were close to opposition. An increased Mach number is observed to cause the Martian BS to move to lower altitudes and the variation in the terminator altitude is proportional to the Mach number change. When the Mach number is lowered, the BS flares more. We also compare our results to previous studies at Venus. The variation in BS altitude with magnetosonic Mach number is found to be very similar to the variation of the Venusian BS, which has previously been shown to decrease linearly in altitude with increasing Mach number.

Citation: Edberg, N. J. T., M. Lester, S. W. H. Cowley, D. A. Brain, M. Fränz, and S. Barabash (2010), Magnetosonic Mach number effect of the position of the bow shock at Mars in comparison to Venus, *J. Geophys. Res.*, **115**, A07203, doi:10.1029/2009JA014998.

1. Introduction

[2] At Mars and Venus, the ionosphere acts as an effective obstacle to the solar wind flow. The flow is thus forced to slow down upstream of the planets and since the solar wind is supersonic (higher bulk velocity than thermal velocity), the solar wind interaction with the ionosphere forms a shock in the flow. This shock, which forms upstream of each planet, is a fast magnetosonic wave. The wave is, however, too slow to travel upstream, and hence becomes a standing wave in the flow, referred to as a bow shock (BS).

[3] The BS has been observed experimentally by several spacecraft at both planets and there are a number of reported studies on them. At Venus, it was first observed on 18 October 1967 by the Venera 4 spacecraft [Dolginov *et al.*, 1968] and a day later by the Mariner 5 spacecraft [Bridge *et al.*, 1967]. Later on, Venera 9 and Venera 10 provided a larger number of crossings, which could be used for statistical studies of the shape and location of the BS [Verigin *et al.*, 1978] and that was further complemented by the many observations conducted by the Pioneer Venus Orbiter (PVO)

during its 14-year-long mission. Lately, Venus Express has also started sampling the BS and is still doing so [Zhang *et al.*, 2007; Martinecz *et al.*, 2008].

[4] At Mars, the BS was first observed by the Mariner 4 spacecraft in 1964 and soon followed by the Mars series of spacecraft that together could be used to derive an initial shape of the Martian BS [Slavin and Holzer, 1981]. Subsequently, Phobos 2 and the Mars Global Surveyor (MGS) significantly increased the number of crossings [Riedler *et al.*, 1989; Vignes *et al.*, 2000], and at present Mars Express (MEX) is continuously sampling the boundary [Edberg *et al.*, 2009].

[5] Besides studying the average shape and location of the BS at each planet, the factors that controlled their locations are a topic of extensive research. At Venus, the BS location was determined to be influenced by the solar activity as the altitude of the boundary was shown to be much lower, on average, when Venera 9 and Venera 10 sampled the boundary during solar minimum compared to when PVO sampled the boundary during solar maximum ($2.14 R_V$ compared to $2.44 R_V$ in the terminator plane, where $1 R_V = 6052$ km) [Slavin *et al.*, 1979]. The influence of the solar wind dynamic pressure was examined by Slavin *et al.* [1980] and was found to have a significant effect. The BS became more compressed as the solar wind dynamic pressure increased. Slavin *et al.* [1980] also studied the influence of the magnetosonic Mach number, M_{MS} , and the Alfvénic Mach number, M_A , and found that they also had a significant effect. In that study, only 18 BS crossings were used. However, Tatrallyay *et al.* [1983] later reproduced those results using a larger data set of crossings from PVO and showed that both the dynamic pressure as well as the Mach

¹Department of Physics and Astronomy, University of Leicester, Leicester, UK.

²Also at Swedish Institute of Space Physics, Uppsala, Sweden.

³Space Sciences Laboratory, University of California, Berkeley, California, USA.

⁴Max Planck Institute for Solar System Research, Katlenburg-Lindau, Germany.

⁵Swedish Institute of Space Physics, Kiruna, Sweden.

numbers (magnetosonic and Alfvénic) had a significant effect on the boundary location.

[6] Using PVO measurements, *Alexander and Russell* [1985] showed that the BS altitude was correlated with the solar cycle and *Alexander et al.* [1986] that the interplanetary magnetic field (IMF) direction made the BS shape asymmetric. After PVO had been in orbit around Venus for more than a full solar cycle, *Russell et al.* [1988] provided further insight into which factors controlled the location of the BS by using a statistical data set of 2000 BS crossings. The BS altitude was, again, clearly seen to vary in concert with the solar cycle variation. The explanation being that the EUV flux increased the ionization around Venus, which added mass to the solar wind flow through pickup of ions such that the solar wind was forced to slow down, thereby creating a larger obstacle; hence, the BS grew larger. The large number of crossings made it possible to separate between cases of low and high solar EUV flux and it was shown that the dynamic pressure had an influence only when the EUV flux was high and the dynamic pressure was low. The magnetosonic Mach number, on the other hand, was shown to always have a strong influence on the BS altitude and hence seemed to be a more important factor [*Russell et al.*, 1988]. Furthermore, the BS shape in the terminator plane was shown to be asymmetric whenever the IMF was perpendicular to the flow direction, an effect that was explained by the anisotropic propagation of the fast magnetosonic wave [*Russell et al.*, 1988]. Several years later, *Zhang et al.* [2004] revisited the PVO measurements and normalized the BS altitude to the magnetosonic Mach number, EUV flux, and IMF direction to show that the BS was, in fact, quite insensitive to solar wind dynamic pressure.

[7] The long-lasting mission of PVO, which carried both a magnetometer and plasma instruments, left few questions unanswered on the location and shape of the BS as well as on which factors controlled it. At Mars, however, the situation was not as fortunate even after several missions to the planet. After Mariner 4 and the 'Mars' series of missions only a handful of BS crossing were completed. Not until Phobos 2 had completed ~50 orbits could some statistics be done on the controlling factors.

[8] The solar wind dynamic pressure was concluded to have only a very weak influence on the Martian BS location as determined by using BS crossings from these 50 orbits from Phobos 2 [*Schwingschuh et al.*, 1992]. The solar cycle effect was shown to be insignificant as the average BS altitude did not change between the time of the Mariner 4 encounter and the 'Mars' series of missions, during solar minimum, and when Phobos 2 observed it during solar maximum [*Slavin et al.*, 1991; *Zhang et al.*, 1991a]. The orientation of the IMF was shown to have an effect as the BS moved to higher altitudes when the IMF direction became closer to being perpendicular to the local normal to the BS [*Zhang et al.*, 1991b].

[9] The number of crossings by Phobos 2 used in the statistics to determine which factors controlled the location of the Martian BS was, however, fairly small (~100). Most results were therefore somewhat uncertain, considering that there are three to four potential factors that influence the position of the boundary at the same time.

[10] After the arrival of MGS in 1997, the studies of the Martian BS could be resumed once again. MGS conducted ~700 crossings of the BS that could be used for larger statistical studies. More accurate models of the shape of the BS soon emerged [*Vignes et al.*, 2000; *Trotignon et al.*, 2006; *Edberg et al.*, 2008]. *Vignes et al.* [2002] showed that the BS was sensitive to the IMF direction, but only if using crossings when the upstream IMF direction could be reliably determined and when it was very steady, which were again no more than ~100 in total. MGS did carry an electron spectrometer instrument but the plasma density, velocity, and temperature could not be routinely obtained from those measurements such that the effect of the solar wind dynamic pressure, the magnetosonic (or the Alfvénic) Mach number, could not be studied.

[11] Furthermore, with the arrival of MGS, another potential factor that could possibly influence the BS location was discovered. MGS measurements showed that Mars did not have a significant dipolelike magnetic field but rather had significant portions of its crust magnetized [*Acuña et al.*, 1998]. *Crider et al.* [2002] showed that the crustal magnetic fields locally pushed the magnetic pileup boundary (MPB) to higher altitudes. *Edberg et al.* [2008] presented evidence that supported that also the BS was influenced but with a small number of crossings as the BS was seldom crossed over the regions of strong crustal magnetization.

[12] Mars Express (MEX) has presently been in orbit around Mars for nearly 6 years and is continuously sampling the BS. Using these measurements, *Dubinin et al.* [2008] showed that the magnetosheath of Mars is on average higher over the southern hemisphere of Mars, where the crustal magnetic fields are stronger. *Edberg et al.* [2009] performed a statistical study of which factors control the Martian BS using the first 5 years of MEX measurements. In that study, the dynamic pressure and the solar EUV flux were found to have an influence on the BS location while the IMF direction had a weak influence. The IMF direction was, however, determined from a proxy using MGS magnetic field measurements of the draped field lines beneath the BS, which introduced some uncertainties. *Edberg et al.* [2009] also showed that there was some influence of the crustal magnetic fields on the BS location, but again, few BS crossings occurred over the strongest crustal sources.

[13] Despite the many missions to Mars, the effect of the magnetosonic Mach number on the Martian BS location has never been properly studied. MGS did not carry an instrument for measuring the solar wind density and velocity and MEX did not carry a magnetometer to measure the IMF strength. *Verigin et al.* [2004] used Phobos 2 measurements to determine that a few, very high altitude, BS crossings at Mars in March 1989 were related to the low Alfvénic Mach number, but no statistical study of the Mach number effect has been conducted using Phobos 2 measurements.

[14] Therefore, in this article we present the result of a statistical study of how the BS varies with the magnetosonic Mach number and compare that to how the BS varies at Venus. The BS altitude is determined from MEX measurements and the Mach number is calculated using solar wind measurements from the Advanced Composition

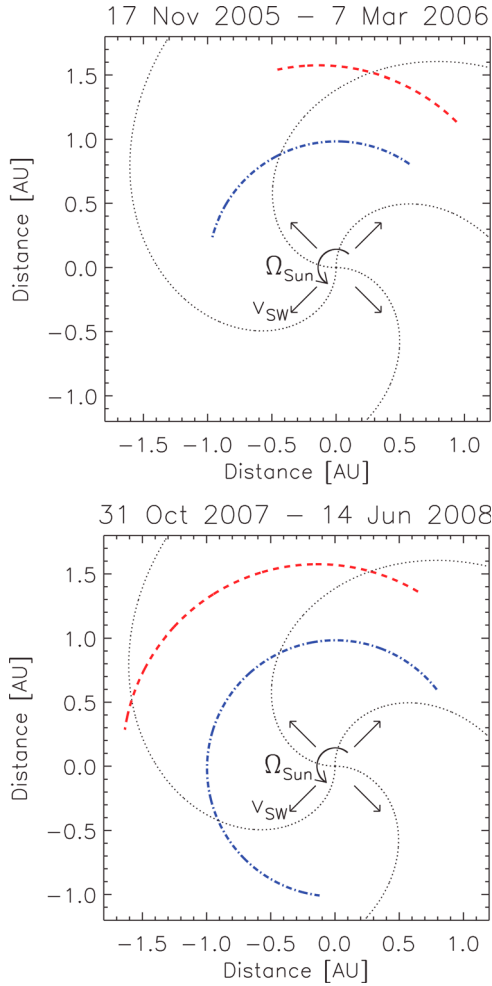


Figure 1. The orbital tracks of Earth (blue dash-dotted line) and Mars (red dashed line) during two intervals when the two planets are approximately aligned on a Parker spiral (dotted line). The Parker spirals shown are constructed assuming a solar wind radial velocity $v_{sw} = 400 \text{ km s}^{-1}$ and a solar angular velocity $\Omega_{Sun} = 2\pi/24 \text{ d}^{-1}$. The data from ACE and MEX during these intervals are used for determining the Mach number effect of the BS altitude.

Explorer (ACE) spacecraft upstream of Earth, extrapolated to Mars.

2. Observations

2.1. ACE Measurements of the Mach Number

[15] ACE orbits the $L1$ Lagrange point upstream of Earth and continuously measures the solar wind proton density, temperature, and velocity, as well as the vector magnetic field but not the electron temperature. The measured upstream solar wind conditions at the Earth are not normally the same as the upstream conditions at Mars. However, this can be the case, approximately, when Mars and Earth are located in approximately the same solar wind sector and the solar wind coming from one region on the Sun is constant in time. Then the solar wind can be assumed to be constant along a Parker spiral line, or a solar wind streamline, and the frozen-in IMF will also coincide with the streamlines. Mars'

and Earth's orbital periods are approximately in a 1:2 resonance to each other and hence are located at similar heliospheric longitudes for a couple of month every 2 years. Depending on the number of solar wind sectors and how much the solar wind plasma streamlines vary in time, extrapolation of solar wind conditions from Earth to Mars will have inherent errors. The magnitude of these errors are difficult to determine but on a statistical level they will most likely even out.

[16] *Vennerstrom et al.* [2003] showed that the magnetic field measured by ACE could be extrapolated to Mars during an interval in 1999 when Mars and Earth were close to being aligned on a Parker spiral. To perform such an extrapolation a time shift, Δt , had to be applied to the ACE measurements. The time shift consists of two terms,

$$\Delta t = \Delta t_1 + \Delta t_2, \quad (1)$$

where

$$\Delta t_1 = \frac{r_{Mars} - r_{Earth}}{v_{sw}} \quad (2)$$

accounts for the time it takes the solar wind with velocity v_{sw} to propagate the radial distance between Mars and Earth, $r_{Mars} - r_{Earth}$, and where

$$\Delta t_2 = \frac{\phi_{Mars} - \phi_{Earth}}{\Omega_{Sun}} \quad (3)$$

accounts for the time it takes the Sun to rotate the angular distance between Mars' and Earth's positions in heliospheric longitude, $\phi_{Mars} - \phi_{Earth}$, with angular velocity $\Omega_{Sun} = 2\pi/24 \text{ d}^{-1}$. Two intervals when Mars and Earth are in the same solar wind sector have occurred since MEX arrived at Mars, starting in 2005 and in 2007. The paths of Mars and Earth during these intervals are illustrated in Figure 1 together with an average Parker spiral configuration. MEX does not cross the BS during every orbit since the precessing orbit of MEX causes the apoapsis to go to lower altitudes than the normal BS altitude during certain seasons. Including this constraint, we are left with the two intervals illustrated in Figure 1 during which we can use ACE data to calculate the magnetosonic Mach number and extrapolate the values to Mars.

[17] When extrapolating the solar wind values to Mars, we assume that the magnetic field and the density both fall off as $1/r^2$, while the electron temperature falls off as $1/r^{1/3}$ and the ion temperature as $1/r^{2/3}$ [Slavin and Holzer, 1981]. Since the electron temperature is not routinely measured by ACE, we use the average value at Earth's orbit of $1.41 \times 10^5 \text{ K}$, as determined by *Newbury et al.* [1998]. Once all parameters have been adjusted in magnitude and the values shifted in time according equations (1)–(3), the magnetosonic Mach number perpendicular to the local IMF direction is calculated as the ratio between the solar wind speed and the magnetosonic speed

$$M_{MS} = \frac{v_{sw}}{\sqrt{v_A^2 + v_S^2}}, \quad (4)$$

where v_{sw} is the solar wind speed and $v_A = B/\sqrt{\rho\mu_0}$ and $v_S = \sqrt{\gamma P/\rho}$ are the Alfvén speed and the sound speed, respectively. B is the magnetic field strength, ρ is the solar wind mass density (assuming 4% helium and 96% protons),

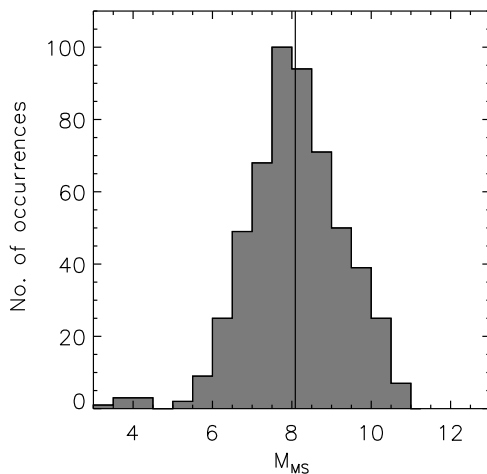


Figure 2. The distribution of the magnetosonic Mach numbers calculated using ACE data and extrapolated to Mars. The mean value of 8.1 is indicated by the vertical line.

μ_0 is the permeability of vacuum, $\gamma = 5/3$ is the ratio of specific heats, and $P = nk_B(T_e + T_i)$ is the solar wind pressure, where n is the solar wind density, k_B is Boltzmann's constant, and T_e and T_i are the electron and ion temperatures, respectively.

[18] The Gaussian distribution of the magnetosonic Mach numbers is shown in Figure 2. The magnetosonic Mach number increases with radial distance from the Sun such that the mean value at Mars is 8.1. Other than the higher mean value, the distribution is fairly similar to the distribution obtained by *Grocott et al.* [2009], their Figure 1, who used data from ACE as well but for a different interval and a different research topic.

2.2. Mars Express Observations of the Bow Shock

[19] The MEX spacecraft is equipped with the Analyzer of Space Plasma and Energetic Atoms (ASPERA-3), which includes an electron sensor (ELS) and an ion mass analyzer (IMA) [Barabash *et al.*, 2006]. ELS measures electrons in the energy range 1 eV–20 keV in a $4^\circ \times 360^\circ$ slit of the sky with a time resolution of 4 s. IMA measures ions in the energy range 10 eV/q–30 keV/q with a field of view of $90^\circ \times 360^\circ$ and a time resolution of typically 192 s. MEX arrived at Mars in late 2003 and was inserted into an elliptical orbit, with apoapsis at $\sim 10,000$ km and periapsis at ~ 300 km, which precesses in local time.

[20] In a time series of inbound ELS data, the BS is observed as a sudden increase of fluxes of electrons at energies between 10 eV and ~ 500 eV. During the initial 5 years of the MEX mission at Mars, 3277 BS crossings were identified by *Edberg et al.* [2009]. This number decreases to 832 when only including crossings that take place during the two intervals specified in Figure 1. Examples of typical BS crossings observed in ELS data can be found in *Edberg et al.* [2009] (their Figures 3–5). The uncertainty in the identification of BS crossings is usually within a few minutes that corresponds, approximately, to no more than 100 km in radial distance.

[21] The orbital evolution of MEX guarantees crossings of the BS at a large range of solar zenith angles (SZA), the

SZA being the angle from the x axis in Mars solar orbital (MSO) system. In the MSO system the x axis is directed along the Mars–Sun line, with the z axis parallel to the Mars orbital momentum vector and the y axis completing the right-handed system. In order to compare the altitude of each individual BS crossing, they first need to be extrapolated to a common SZA since there is a strong dependence on the BS altitude with SZA. Figure 3a shows the distance of the BS crossings normalized to the planetary radii, R_M ($1 R_M = 3397$ km), as a function of SZA. The increase in distance with increasing SZA is obvious. The position of the crossings have first been accounted for the mean 4° aberration of the solar wind direction caused by the orbital motion of the planet. In Figure 3b the crossings are extrapolated to the terminator plane (SZA = 90°) before being plotted as a function of SZA. The dependence on SZA is now less significant. The extrapolation to the terminator plane is done in the same way as by, e.g., *Vignes et al.* [2002], where the best fit average shape (a conic section) of the BS is adjusted in its radius to fit each single BS crossing. The terminator distance is then calculated from each conic section. As can be seen in Figure 3b there is a lot of scatter in the BS terminator distance, which illustrates the variability of this boundary. For a SZA of 90° the boundary distance can vary by $\sim 1 R_M$, depending on the upstream conditions such as the magnetosonic Mach number.

2.3. The Magnetosonic Mach Number Effect on the Bow Shock

[22] In Figure 4 the BS distances, extrapolated to the terminator plane, are plotted as a function of magnetosonic Mach number. The mean of the terminator distances are

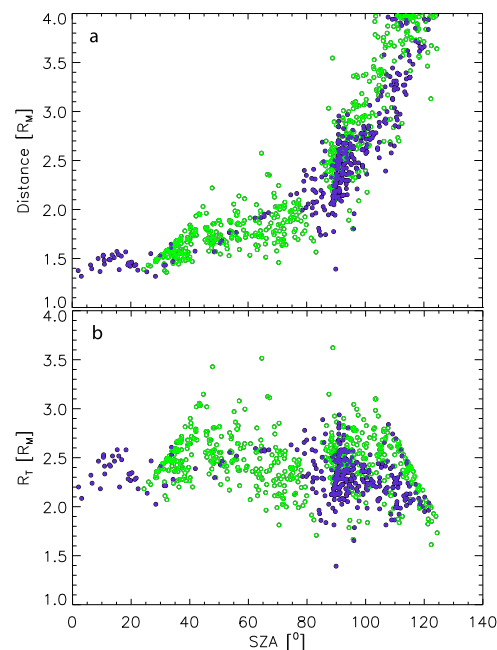


Figure 3. (a) The distances of the BS crossings observed by MEX during the first (green circles) and the second (purple filled circles) intervals in Figure 1 as a function of SZA and (b) the distances of the same BS crossings extrapolated to the terminator plane, R_T , as a function of SZA.

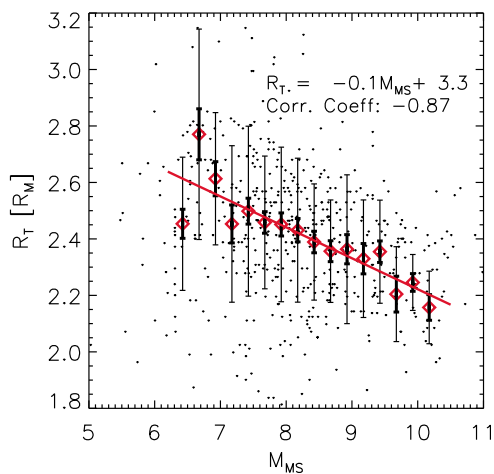


Figure 4. The extrapolated terminator distance of the BS plotted as a function of the magnetosonic Mach number (dots). The mean values of the terminator distances in Mach number bins of 0.25 (red diamonds) and the standard deviation in each bin are shown (thin error bars) together with the standard error on the mean (thick error bars). A linear least-squares fit is done to the mean values (solid red line) with the equation shown at the top of the plot together with the correlation coefficient of the mean values. Only crossings in the SZA range 40° – 110° are included to avoid any orbital coverage bias.

calculated in Mach number bins of 0.25, ranging from Mach number 6.1 to 10.5. Outside of this interval there are few data points in each bin (<10) such that we do not include them. A linear curve is least-squares fitted to the mean values and there is a clear trend of a lower BS altitude for an increasing Mach number. We exclude the crossings that take place outside the SZA range 40° – 110° to avoid any orbital bias. If including crossings from all SZAs the results differ somewhat, as the value of the slope of the linear fit changes by ~ 0.02 (0.1 to 0.08).

[23] Since there is an (unknown) source of error included in the extrapolation of the BS distance to the terminator plane, we also show the Mach number effect on the BS in another way. In Figure 5 the mean unextrapolated BS distances calculated in four SZA intervals ranging from 10° to 120° are plotted for high (>9.0) and low (<7.0) Mach number (8.1 being the average Mach number). Conic sections, $r = L/[1 + \epsilon \cos(\theta)]$, where r and θ are the polar coordinates referenced to the x axis in the MSO system and centered at $(X_0, 0, 0)$, ϵ is the eccentricity, and L is the semilatus rectum, are then fitted to the mean values to display the BS shape during low Mach number solar wind in relation to the shape during high Mach number solar wind. The average shape of the BS as determined from crossings from the entire first 5 years of the MEX mission is also shown as a reference. Clearly, when the Mach number is higher than average, the BS becomes compressed, while the shape, on the other hand, does not change significantly compared to the average shape. The BS altitude rather seems to be uniformly lowered at all SZAs. When the Mach number drops, the BS moves to higher altitudes and the shape also changes. The flaring of the BS increases with

decreasing Mach number as the mean distances at higher SZAs increase more than the mean distances at lower SZA.

3. Comparison to Venus

[24] The global plasma environments at Mars and Venus, which are influenced by the solar wind interaction, are in general quite similar. Venus has a denser atmosphere and is larger in size with a higher gravity than Mars, which introduces some differences. Also, Mars is farther away from the Sun such that the solar wind conditions differ compared to those at Venus. Strong crustal magnetic fields exist at Mars, which distort the solar wind interaction somewhat, whereas Venus does not have any significant magnetic fields. Nevertheless, the shape and location of the BS at the two planets are very similar.

[25] The BS at Venus is on average at a lower terminator distance than the BS at Mars when normalized to the planetary radius ($2.3 R_V$ compared to $2.6 R_M$). The BS at Venus has been shown empirically to be sensitive to EUV flux, the solar cycle phase, and, to some extent, the IMF direction but not as much to solar wind dynamic pressure [Russell *et al.*, 1988]. The BS at Mars has in the same manner been shown to be sensitive to EUV flux but also to the dynamic pressure. The crustal magnetic fields affect the BS at Mars to some extent while the IMF direction does not seem to play an equally strong role [Edberg *et al.*, 2009]. The difference in sensitivity to the IMF direction is surprising and could possibly be explained by the difference in obstacle size of the two planets compared to the ion gyro-

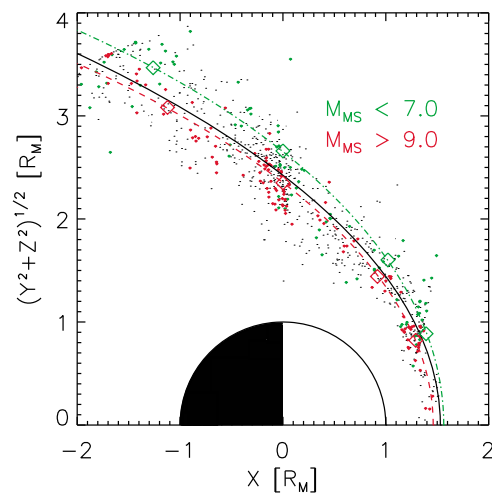


Figure 5. The shape of the BS during high ($M_{MS} > 9.0$) and low ($M_{MS} < 7.0$) magnetosonic Mach number (red and green lines, respectively) shown in cylindrical MSO coordinates. The positions of the BS crossings during high and low Mach number (red and green dots, respectively) are displayed together with the average distances within four SZA ranges (red and green diamonds). The two shapes of the BS are obtained by fitting conic sections to the average distances. The average shape derived from all the BS crossings observed by MEX during 2004–2008 is shown as a reference (black line) and all the BS crossing from the two intervals in Figure 1 are shown as black dots.

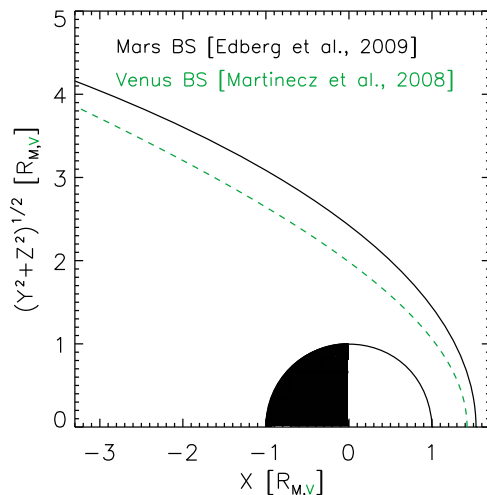


Figure 6. The average shapes of the BS at Venus (green dashed line) and at Mars (solid line) normalized to planetary radius. The boundaries take the shape of conic sections as described in the text, with parameters $L = 1.303$, $\epsilon = 1.056$ and $X_0 = 0.788$ for the Venus BS and $L = 1.98$, $\epsilon = 0.96$ and $X_0 = 0.52$ for the Mars BS.

radius or the fact the the direction of the IMF is not reliably determined at Mars.

[26] The effect of the magnetosonic Mach number on the Martian BS in this study has been shown to be quite similar to the effect on the Venus BS. *Russell et al.* [1988] showed that the Venusian terminator BS distance is lowered when the Mach number increases. The BS terminator distance seems to fall off linearly [*Russell et al.*, 1988, Figure 9]. In this study we find a similar relation as the Martian BS also falls off linearly with increasing Mach number. Even though gas dynamic modeling suggests that the BS terminator distance should fall off in a more exponential fashion [*Tatallyay et al.*, 1984], this does not seem to be the case at Mars or Venus. *Russell et al.* [1988] suggested that this discrepancy between model and observations at Venus was caused by added mass loading of the solar wind. The mass loading of the solar wind creates a bigger obstacle which in turn affects the BS shape. This explanation is equally plausible at Mars.

[27] In our statistical study, we have been limited to Mach numbers between 6.1 and 10.5. However, the Mach number can, of course, be smaller, or larger, than this. *Verigin et al.* [2004] studied a couple of events in Phobos 2 data from 24 March 1989 when the BS at Mars was located at extremely large distances ($\sim 10 R_M$) upstream of the planet. The large distance was attributed to the unusually low Alfvénic Mach number at this time, in combination with the low solar wind dynamic pressure. At Venus, extremely distant ($\sim 12 R_V$) BS encounters have been reported by *Russell and Zhang* [1992] and *Zhang et al.* [2008], which have been associated with magnetosonic Mach numbers close to 1. Occasional extreme BS distances seem to occur at both planets. Of course, these extreme values do not agree with the result obtained here or by *Russell et al.* [1988], where the BS altitude increases linearly with falling magnetosonic Mach number. Since we do not have many

samples of BS crossings at very low solar Mach numbers (below 6.1) we cannot say for sure if the BS distance continues to increase in proportion to a decreasing Mach number or if it rather starts to increase exponentially, which the extreme case studies imply.

[28] One significant difference between Mars and Venus is, of course, that the average Mach numbers at Venus are lower than those at Mars (by about 3.6). The Venusian BS is also at a higher altitude. However, Venus has twice the radius of Mars and the magnetospheric obstacle at Venus is approximately twice as large as that at Mars, which strongly affects the BS shape and location. Normalizing to planetary radius, the differences in location between Mars' and Venus' BS are then reversed. Figure 6 shows the average conic section shape of the BS at Mars and Venus normalized to planetary radius from the studies by *Edberg et al.* [2009] and *Martinecz et al.* [2008]. The Venusian BS is clearly at lower altitudes than the BS at Mars as has been reported in previous comparisons [*Slavin and Holzer*, 1981] (their Figure 20). The Venusian BS crossings, which the average shape is based on, were gathered by Venus Express at solar minimum during five months in 2008 and the BS crossings at Mars were gathered by MEX from 2004 until 2009, which is on the declining phase of the solar cycle.

4. Discussion

[29] Using ACE data at Earth to infer the solar wind conditions at Mars seems to be a valid technique on a statistical level, at least $\sim 10\%$ – 15% of the time, when Mars and Earth are close to opposition. There are, of course, uncertainties involved, which include how the solar wind parameters vary as they propagate from Earth to Mars, but on a statistical level it seems to work. There is a fair amount of scatter in the position of the crossings when plotted versus the Mach number and some of this scatter is likely to be caused by the error in extrapolating the Mach number to Mars. A smaller error is also introduced when the electron temperature is assumed constant when calculating the Mach number.

[30] We have shown that the magnetosonic Mach number, as calculated from ACE data and extrapolated to Mars, has a strong influence on the Martian BS. The BS, being a standing fast magnetosonic wave, takes the form of a conic, to a first approximation, which is shaped according to the ratio of the solar wind speed to the magnetosonic speed. When the magnetosonic Mach number is higher than average, the BS is at lower distances than average, and consequently, when the Mach number is low, the BS distance is high. The terminator BS distance is in this article found to be related to the Mach number as

$$R_T = -0.1M_{MS} + 3.3. \quad (5)$$

The BS distance hence falls off linearly with increasing Mach number.

[31] The extrapolated terminator distance in Figure 4 changes by $\sim 0.4 R_M$ when the Mach number changes from 6.5 to 10.5. The fitted curves in Figure 5 suggest a difference in terminator distance of ~ 0.3 when the Mach number is lower than 7.0 compared to when the Mach number is

higher than 9.0. These changes in distance with changing Mach number from the two methods are quite consistent.

[32] The flaring of the BS increases when the Mach number is lowered such that the terminator BS distance undergoes larger changes in distance than the subsolar BS when the Mach number changes.

[33] The variation of the BS distance with Mach number at Mars is found to be very similar to that at Venus. The BS at each planet varies in proportion to the Mach number and they can both be at extreme distances when the Mach number is extremely low.

[34] Despite the smaller obstacle radius, the BS of Mars seems to be affected by the magnetosonic Mach number in the same way as Venus' BS, thereby giving further justification to using MHD theory when studying the solar wind interaction with Mars. The results presented in this article give some further implications for how the BSs of other solar system bodies are expected to react to varying Mach number. The BS of, for example, Mercury might very well be affected in the same way since the obstacle size is similar to that of Venus and Mars. This is something that will be possible to determine after the arrival of the BepiColombo mission to Mercury. The BS upstream of a comet like 67 P/Churyomov-Gerasimenko, which is the target of the Rosetta mission, would be expected to increase in size as the comet approaches the Sun partly because the Mach number decreases when moving inward in the solar system. On the other hand, the BS of Pluto, if any ionospheric obstacle to the solar wind exists there, would be expected to be very small since the solar wind Mach number is very high at such distances from the Sun. The New Horizons spacecraft might be able to investigate this in the future.

[35] **Acknowledgments.** N.J.T.E. was supported by the European Union 6th Framework, contract MEST-CT-2004-7512. M.L. and S.W.H. C. were supported by STFC grant PP/E000983/1.

[36] Masaki Fujimoto thanks Tielong Zhang and another reviewer for their assistance in evaluating this article.

References

- Acuña, M. H., et al. (1998), Magnetic field and plasma observations at Mars: Initial results of the Mars Global Surveyor mission, *Science*, **279**, 1676–1680.
- Alexander, C. J., and C. T. Russell (1985), Solar cycle dependence of the location of the Venus bow shock, *Geophys. Res. Lett.*, **12**, 369–371, doi:10.1029/GL012i006p00369.
- Alexander, C. J., J. G. Luhmann, and C. T. Russell (1986), Interplanetary field control of the location of the Venus bow shock: Evidence for comet-like ion pickup, *Geophys. Res. Lett.*, **13**, 917–920, doi:10.1029/GL013i009p00917.
- Barabash, S., et al. (2006), The analyzer of space plasmas and energetic atoms (ASPRA-3) for the Mars Express mission, *Space Sci. Rev.*, **126**, 113–164, doi:10.1007/s11214-006-9124-8.
- Bridge, H. S., A. J. Lazarus, C. W. Snyder, E. J. Smith, L. Davis, P. J. Coleman Jr., and D. E. Jones (1967), Mariner V: Plasma and magnetic fields observed near Venus, *Science*, **158**, 1669–1673, doi:10.1126/science.158.3809.1669.
- Crider, D. H., et al. (2002), Observations of the latitude dependence of the location of the martian magnetic pileup boundary, *Geophys. Res. Lett.*, **29**(L8), 1170, doi:10.1029/2001GL013860.
- Dolginov, S. S., E. G. Eroshenko, and D. N. Zhuzgov (1968), Magnetic field investigation with interplanetary station “Venera-4”, *Cosmic Research*, **6**, 469.
- Dubinin, E., G. Chanteur, M. Fraenz, R. Modolo, J. Woch, E. Roussos, S. Barabash, R. Lundin, and J. D. Winningham (2008), Asymmetry of plasma fluxes at Mars. ASPERA-3 observations and hybrid simulations, *Planet. Space Sci.*, **56**, 832–835, doi:10.1016/j.pss.2007.12.006.
- Edberg, N. J. T., M. Lester, S. W. H. Cowley, and A. I. Eriksson (2008), Statistical analysis of the location of the martian magnetic pileup boundary and bow shock and the influence of crustal magnetic fields, *J. Geophys. Res.*, **113**, A08206, doi:10.1029/2008JA013096.
- Edberg, N. J. T., D. A. Brain, M. Lester, S. W. H. Cowley, R. Modolo, M. Fränz, and S. Barabash (2009), Plasma boundary variability at Mars as observed by Mars global surveyor and Mars express, *Ann. Geophys.*, **27**(9), 3537–3550.
- Grocott, A., S. V. Badman, S. W. H. Cowley, S. E. Milan, J. D. Nichols, and T. K. Yeoman (2009), Magnetosonic Mach number dependence of the efficiency of reconnection between planetary and interplanetary magnetic fields, *J. Geophys. Res.*, **114**, A07219, doi:10.1029/2009JA014330.
- Martinez, C., et al. (2008), Location of the bow shock and ion composition boundaries at Venus—initial determinations from Venus Express ASPERA-4, *Planet. Space Sci.*, **56**, 780–784, doi:10.1016/j.pss.2007.07.007.
- Newbury, J. A., C. T. Russell, J. L. Phillips, and S. P. Gary (1998), Electron temperature in the ambient solar wind: Typical properties and a lower bound at 1 AU, *J. Geophys. Res.*, **103**(A5), 9553–9566, doi:10.1029/98JA00067.
- Riedler, W., K. Schwingenschuh, D. Moehlmann, V. N. Oraevskii, E. Eroshenko, and J. Slavin (1989), Magnetic fields near Mars: First results, *Nature*, **341**, 604–607, doi:10.1038/341604a0.
- Russell, C. T., and T.-L. Zhang (1992), Unusually distant bow shock encounters at Venus, *Geophys. Res. Lett.*, **19**, 833–836, doi:10.1029/92GL00634.
- Russell, C. T., E. Chou, J. G. Luhmann, P. Gazis, L. H. Brace, and W. R. Hoegy (1988), Solar and interplanetary control of the location of the Venus bow shock, *J. Geophys. Res.*, **93**, 5461–5469, doi:10.1029/JA093iA06p05461.
- Schwingenschuh, K., W. Riedler, T.-L. Zhang, H. Lichtenegger, H. Rosenbauer, S. Livi, G. Gevai, K. Gringauz, M. Verigin, and E. Eroshenko (1992), The Martian magnetic field environment - Induced or dominated by an intrinsic magnetic field?, *Adv. Space Res.*, **12**, 213–219, doi:10.1016/0273-1177(92)90333-S.
- Slavin, J. A., and R. E. Holzer (1981), Solar wind flow about the terrestrial planets. I - Modeling bow shock position and shape, *J. Geophys. Res.*, **86**(A13), 11,401–11,418.
- Slavin, J. A., R. C. Elphic, and C. T. Russell (1979), A comparison of Pioneer Venus and Venera bow shock observations: Evidence for a solar cycle variation, *Geophys. Res. Lett.*, **6**, 905–908, doi:10.1029/GL006i011p00905.
- Slavin, J. A., R. C. Elphic, C. T. Russell, F. L. Scarf, J. H. Wolfe, J. D. Mihalov, D. S. Intriligator, L. H. Brace, H. A. Taylor, and R. E. Daniell (1980), The solar wind interaction with Venus: Pioneer Venus observations of bow shock location and structure, *J. Geophys. Res.*, **85**, 7625–7641, doi:10.1029/JA085iA13p07625.
- Slavin, J. A., K. Schwingenschuh, W. Riedler, and E. Eroshenko (1991), The solar wind interaction with Mars: Mariner 4, Mars 2, Mars 3, Mars 5, and PHOBOS 2 observations of bow shock position and shape, *J. Geophys. Res.*, **96**(A7), 11,235–11,241.
- Tatallay, M., C. T. Russell, J. D. Mihalov, and A. Barnes (1983), Factors controlling the location of the Venus bow shock, *J. Geophys. Res.*, **88**(A7), 5613–5621, doi:10.1029/JA088iA07p05613.
- Tatallay, M., C. T. Russell, J. G. Luhmann, A. Barnes, and J. D. Mihalov (1984), On the proper Mach number and ratio of specific heats for modeling the Venus bow shock, *J. Geophys. Res.*, **89**(A9), 7381–7392, doi:10.1029/JA089iA09p07381.
- Troignon, J. G., C. Mazelle, C. Bertucci, and M. H. Acuña (2006), Martian shock and magnetic pile-up boundary positions and shapes determined from the Phobos 2 and Mars Global Surveyor data sets, *Planet. Space Sci.*, **54**, 357–369, doi:10.1016/j.pss.2006.01.003.
- Vennerstrom, S., N. Olsen, M. Purucker, M. H. Acuña, and J. C. Cain (2003), The magnetic field in the pile-up region at Mars, and its variation with the solar wind, *Geophys. Res. Lett.*, **30**(7), 1369, doi:10.1029/2003GL016883.
- Verigin, M. I., K. I. Gringauz, T. Gombosi, T. K. Breus, V. V. Bezrukhikh, A. P. Remizov, and G. I. Volkov (1978), Plasma near Venus from the Venera 9 and 10 wide-angle analyzer data, *J. Geophys. Res.*, **83**(A8), 3721–3728, doi:10.1029/JA083iA08p03721.
- Verigin, M. I., J. Slavin, A. Szabo, G. A. Kotova, A. P. Remizov, H. Rosenbauer, S. Livi, K. Szegö, M. Tatallay, K. Schwingenschuh, and T.-L. Zhang (2004), Unusually distant bow shock encounters at Mars: Analysis of March 24, 1989 event, *Space Sci. Rev.*, **111**, 233–243, doi:10.1023/B:SPAC.0000032713.86796.d1.
- Vignes, D., C. Mazelle, H. Reme, M. H. Acuña, J. E. P. Connerney, R. P. Lin, D. L. Mitchell, P. Cloutier, D. H. Crider, and N. F. Ness

- (2000), The solar wind interaction with Mars: locations and shapes of the bow shock and the magnetic pile-up boundary from the observations of the MAG/ER experiment onboard Mars Global Surveyor, *Geophys. Res. Lett.*, *27*(1), 49–52, doi:10.1029/1999GL010703.
- Vignes, D., M. H. Acuña, J. E. P. Connerney, D. H. Crider, H. Rème, and C. Mazelle (2002), Factors controlling the location of the bow shock at Mars, *Geophys. Res. Lett.*, *29*(9), 1328, doi:10.1029/2001GL014513.
- Zhang, T. L., K. Schwingenschuh, H. Lichtenegger, W. Riedler, and C. T. Russell (1991a), Interplanetary magnetic field control of the Mars bow shock: Evidence for Venuslike interaction, *J. Geophys. Res.*, *96*(A7), 11,265–11,269.
- Zhang, T.-L., K. Schwingenschuh, C. T. Russell, and J. G. Luhmann (1991b), Asymmetries in the location of the Venus and Mars bow shock, *Geophys. Res. Lett.*, *18*(2), 127–129, doi:10.1029/90GL02723.
- Zhang, T. L., K. K. Khurana, C. T. Russell, M. G. Kivelson, R. Nakamura, and W. Baumjohann (2004), On the venus bow shock compressibility, *Adv. Space Res.*, *33*, 1920–1923, doi:10.1016/S0273-1177(04)00032-8.
- Zhang, T. L., et al. (2007), Little or no solar wind enters Venus' atmosphere at solar minimum, *Nature*, *450*, 654–656, doi:10.1038/nature06026.
- Zhang, T. L., et al. (2008), Venus Express observations of an atypically distant bow shock during the passage of an interplanetary coronal mass ejection, *J. Geophys. Res.*, *113*, E00B12, doi:10.1029/2008JE003128.
- S. Barabash, Swedish Institute of Space Physics, Kiruna, SE-98128, Sweden. (stas@irf.se)
- D. A. Brain, Space Sciences Laboratory, University of California, 7 Gauss Way, Berkeley, CA 94720, USA. (brain@ssl.berkeley.edu)
- S. W. H. Cowley, N. J. T. Edberg, and M. Lester, Department of Physics and Astronomy, University of Leicester, Leicester LE1 7RH, UK. (swhc1@ion.le.ac.uk; ne@irfu.se; mle@ion.le.ac.uk)
- M. Fränz, Max Planck Institute for Solar System Research, Katlenburg-Lindau, D-37191, Germany. (fraenz@mps.mpg.de)